Y/C separation of composite color video signals using samples with non-opposite sub-carrier phases

Nico Cordes and Gerard de Haan

Philips Research Labs, Video Processing and Visual Perception Group,
Prof. Holstlaan 4, Eindhoven, The Netherlands

ABSTRACT

For analog color television standards such as PAL and NTSC, the transmission of color (C) takes place within the band available for the luminance (Y). At the television receiver, the required separation of Y and C can only be imperfect as both components now share the same frequency space. Modern televisions apply so-called comb-filters that exploit the opposite sub-carrier phase of correlated samples to separate both components. However, cross-talk artifacts and loss of resolution will occur in situations where no sufficiently correlated samples meet the strict opposite phase requirement. In this paper, a novel Y/C separation method is presented that is able to use samples with non-opposite sub-carrier phases.

Keywords: luminance chrominance separation; y/c separation; comb filters; composite video; video signal processing

1. INTRODUCTION

With HDTV sets becoming readily available in many markets, digital television is rapidly gaining popularity. However, analog television is expected to remain an important television standard for several years to come. With the introduction of increasingly larger television sets that exhibit significantly higher resolutions, a continued quality improvement of the decoded analog television signal is desirable.

Many artifacts that continue to exist in analog television are caused by the imperfect separation of luminance and chrominance in composite color video signals. This is due to the fact that for the transmission of PAL, NTSC and SECAM signals, the requirement of backward compatibility to existing black-and-white televisions dictates that the transmission of color (*chrominance*, C) has to take place within the band available for the luminance (Y). At the television receiver, the required separation of Y and C can only be imperfect as both components now share the same frequency space.

This paper introduces a novel method for the Y/C separation of PAL composite color video signals. As the Y/C separation of NTSC signals is very similar, the same method can be used for NTSC with minor adaptations. The Y/C separation of SECAM signals differs fundamentally from that of PAL and NTSC, and is therefore outside the scope of this paper.

For PAL, the chrominance components U and V are amplitude modulated in quadrature onto a sub-carrier with a frequency of 4.43MHz. The resulting one-dimensional spectrum of the composite PAL video signal is illustrated in Figure 1. In addition, the sign of the V-component is inverted every other line, the so-called *V-switch*, to reduce the influence of phase errors.[1] More formally, the above is described in Equation 1, where $\vec{x}$ indicates the pixel position in a given field n, F_{sc} the sub-carrier frequency and F the resulting composite PAL signal.

$$F(\vec{x},n) = Y(\vec{x},n) + U(\vec{x},n)\cdot sin(2\pi F_{sc}t) \pm V(\vec{x},n)\cdot cos(2\pi F_{sc}t) \quad (1)$$

Further author information: (Send correspondence to Nico Cordes)
Nico Cordes: E-mail: Nico.Cordes@philips.com
Gerard de Haan: E-mail: G.de.Haan@philips.com

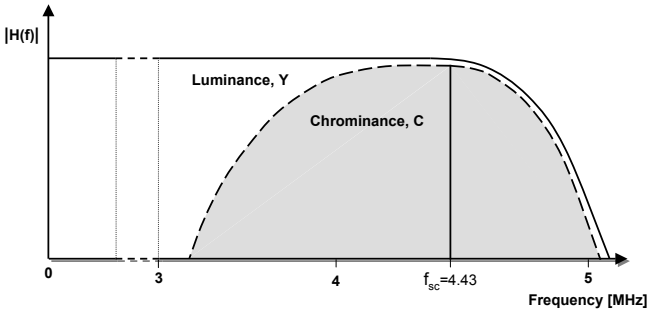

Figure 1. Spectrum of the composite PAL video signal.

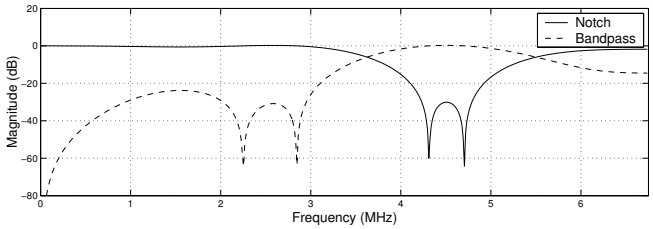

Figure 2. Typical PAL luminance notch and chrominance band-pass filters.

1.1. Early decoders

The early decoders for PAL and NTSC composite video signals used two simple 1D horizontal filters to separate luminance and chrominance from the composite signal. The typical amplitude frequency response of these filters, i.e. the notch and band-pass filters, is shown in Figure 2.

In the luminance path, a notch filter suppresses frequencies near the sub-carrier frequency to eliminate horizontal chrominance components. It can be seen that due to the small stop band of the notch filter, high-frequency chrominance components, as they occur on horizontal colored transitions, are attenuated insufficiently. This introduces cross-talk of chrominance in the luminance, resulting in the so-called *cross-luminance* artifacts. Furthermore, the luminance resolution is significantly reduced, as the notch filter suppresses high luminance frequencies.

In the chrominance path, a band-pass filter separates the high frequency components from the composite signal. Although the passband of the band-pass filter contains mostly chrominance information, high-frequency luminance is present as well. Again, cross-talk will occur as the high-frequency luminance will be decoded as chrominance, resulting in the so-called *cross-color* artifacts.

The above band-pass and notch filters can achieve perfect Y/C separation if the luminance and chrominance values of horizontally adjacent samples are identical, as here the frequency spectrum consists of a DC luminance component and a high frequency chrominance component at the sub-carrier frequency. However, if the correlation along the horizontal axis is insufficient, the frequency spectrum contains high-frequency luminance and chrominance components. The separation is now imperfect, which results in cross-talk artifacts in the decoded signal.

1.2. Comb-filters

In areas where horizontally adjacent samples are insufficiently correlated, improved methods for Y/C separation are desirable. For that purpose, so-called *comb-filters* have been proposed[2] to separate luminance and chrominance along the vertical or temporal axis. Their underlying principles are similar to those of the standard decoder, i.e. passing the desired frequency components and suppressing the undesired frequency components.

However, the luminance and chrominance are now modulated with harmonics of f_h, i.e. the line frequency, and f_v, i.e. the picture frequency. Along with the chosen sub-carrier frequencies of PAL and NTSC, this results in interleaved and non-overlapping luminance and chrominance frequency components in the direction where sufficient correlation is present. For example, in non-moving areas of the picture, the samples are highly correlated along the temporal axis, and as such, the luminance and chrominance components are interleaved and non-overlapping along that axis. A filter with a comb-shaped amplitude response in that particular direction can therefore be used to separate the luminance and chrominance. An example of such a filter is shown in Figure 3.

Comb-filters use two samples with an opposite relative phase, i.e. having a phase difference of 180°, to separate luminance and chrominance. This can be illustrated by taking a composite sample, F_1, that is encoded at an arbitrary phase ϕ:

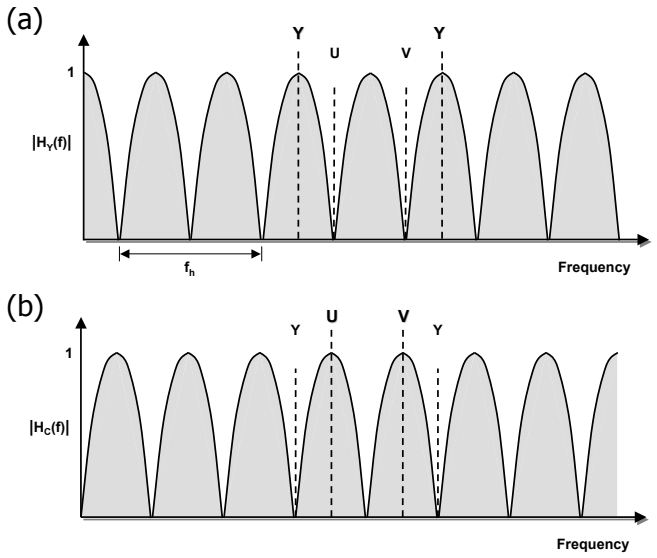

Figure 3. Example of the amplitude frequency response of a PAL comb-filter for a) luminance path, and b) chrominance path.

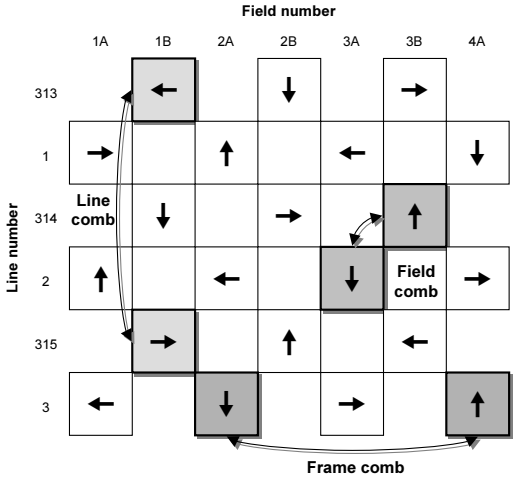

Figure 4. Sub-carrier phase in vertical and temporal direction for PAL signals. Here, the arrow equals the sub-carrier phase, i.e. pointing up denotes 0°. Indicated are the standard comb-filters: line, field and frame.

$$F_1 = Y + U \cdot sin(\phi) + V \cdot cos(\phi) \tag{2}$$

and a second sample F_2, encoded at ϕ+180°, of which we assume that it was encoded from identical luminance and chrominance values as F_1:

$$\begin{aligned} F_2 &= Y + U \cdot sin(\phi + 180°) + V \cdot cos(\phi + 180°) \\ &= Y - U \cdot sin(\phi) - V \cdot cos(\phi) \end{aligned} \tag{3}$$

Now, the average of F_1 and F_2 results in the separated luminance Y, whereas the difference $F_1 - F_2$ divided by two yields the modulated chrominance $U \cdot sin(\phi) + V \cdot cos(\phi)$. The above method can only be applied to PAL if the V-switch of both samples is identical. However, comb-filtering is also possible if the V-switch of both samples differs. In that case, an opposite absolute phase, i.e. $-\phi$, is required for F_2, and again the luminance and chrominance can be separated by addition and subtraction:

$$\begin{aligned} F_2 &= Y + U \cdot sin(-\phi) - V \cdot cos(-\phi) \\ &= Y - U \cdot sin(\phi) - V \cdot cos(\phi) \end{aligned} \tag{4}$$

However, *perfect* separation is only possible if both composite samples were encoded from *identical* Y, U and V values. Only in this case, the positions of the luminance and chrominance frequency components correspond to those of the comb-filter. Therefore, sufficient correlation is required along the comb-filtering direction in order to prevent decoding errors. This is analogous to the horizontal band-pass/notch filters, where sufficient correlation is required along the horizontal axis.

Current state-of-the-art comb-filters adaptively combine various spatial and temporal comb-filters[3],[4] as illustrated in Figure 4, by filtering along the direction of the highest detected correlation. Furthermore, comb-filters have been proposed that apply motion compensation to further increase the temporal correlation[5].[6] However,

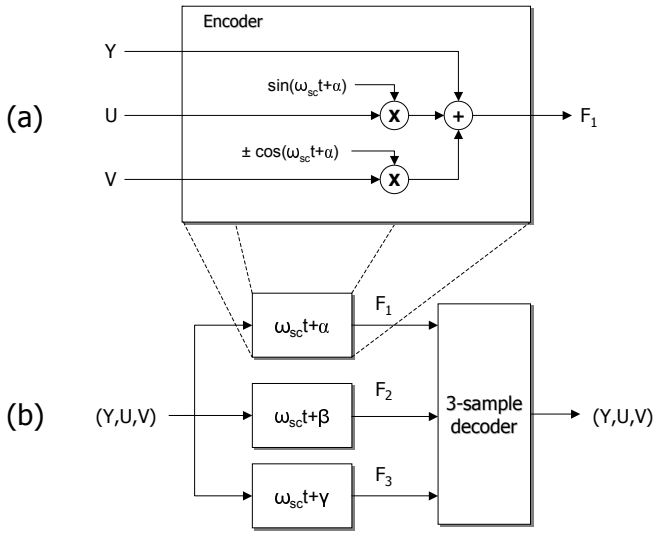

Figure 5. Block diagram of the three-sample decoder.

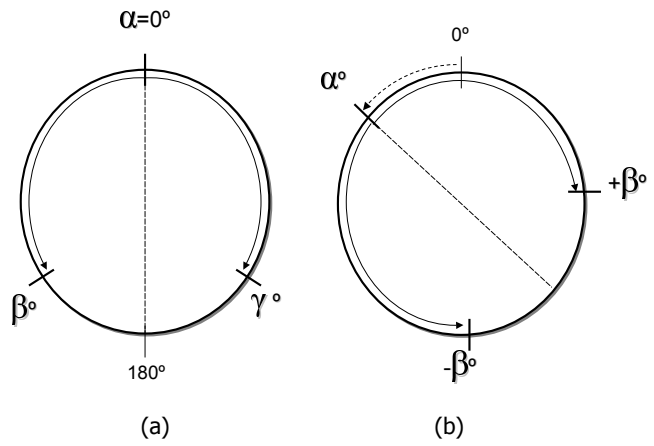

Figure 6. a) Varying relative phases β and γ with respect to a fixed absolute phase α of 0°, and b) varying relative phase β with respect to a varying absolute phase α.

an inherent drawback of the standard comb-filter is the low density of samples that both meet the required phase relationship, and are spatially and/or temporally adjacent. Due to this limited set of samples, situations will occur where neither of the neighboring samples exhibit sufficient correlation with respect to the current sample, thereby causing artifacts in the decoded video. As such, even modern 3D comb-filters suffer from cross-talk artifacts and loss of resolution.

2. NOVEL DECODING PRINCIPLE

To achieve a further reduction in cross-talk artifacts, the possible decoding options need to be expanded. A new option results from using samples with a non-opposite phase relationship with respect to the current sample. If these samples could be used for decoding, the number of decoding options in a given spatial/temporal volume of the sequence could be greatly expanded.

In the PAL decoder, a received composite sample, $F(\vec{x}, n)$, introduces three unknown variables, Y, U and V, and one known value ωt, the locally regenerated sub-carrier phase. Basic algebra learns that, given three linear equations, these three unknown variables can be solved. This means that three composite samples, encoded from *identical* Y, U and V values, can be used to separate the Y, U and V components exactly.

2.1. Principles

To discuss the decoding of samples with non-opposite phases in more detail, two situation with respect to the V-switch of the three composite samples should be considered:

- The V-switch of all three samples is identical.
- One of the three samples has an unequal V-switch with respect to the other samples.

As the difference is restricted to an alternating sign of the V-component, the decoding principles discussed below are highly similar and hence only worked out in detail for samples with identical V-switches.

In case of identical V-switches, consider three composite samples encoded from the same Y, U and V values as shown in Equation 5. In order to obtain three independent equations, the phases were chosen to be unequal, i.e. $\alpha \neq \beta \neq \gamma$. Also, the V-switch of all V components is chosen to be positive. In case of all negative V-switches, the situation is identical expect for an inversion of the sign of the decoded V component.

$$\begin{aligned} F_1 &= Y + U \cdot sin(\alpha) + V \cdot cos(\alpha) \\ F_2 &= Y + U \cdot sin(\beta) + V \cdot cos(\beta) \\ F_3 &= Y + U \cdot sin(\gamma) + V \cdot cos(\gamma) \end{aligned} \tag{5}$$

By solving these three linear equations for the Y, U and V components, the expressions in Equations 6 and 7 are obtained. Here, the Y, U and V components are expressed in terms of the three original composite samples and their corresponding sub-carrier phase.

$$\begin{aligned} Y_n &= +F_1 \cdot sin(\beta) \cdot cos(\gamma) - F_1 \cdot sin(\gamma) \cdot cos(\beta) \\ &\quad +F_2 \cdot sin(\gamma) \cdot cos(\alpha) - F_2 \cdot sin(\alpha) \cdot cos(\gamma) \\ &\quad +F_3 \cdot sin(\alpha) \cdot cos(\beta) - F_3 \cdot sin(\beta) \cdot cos(\alpha) \\ U_n &= +F_1 \cdot cos(\beta) - F_1 \cdot cos(\gamma) + F_2 \cdot cos(\gamma) \\ &\quad -F_2 \cdot cos(\alpha) + F_3 \cdot cos(\alpha) - F_3 \cdot cos(\beta) \\ V_n &= +F_1 \cdot sin(\gamma) - F_1 \cdot sin(\beta) + F_2 \cdot sin(\alpha) \\ &\quad -F_2 \cdot sin(\gamma) + F_3 \cdot sin(\beta) - F_3 \cdot sin(\alpha) \\ D &= +sin(\alpha) \cdot cos(\beta) - sin(\alpha) \cdot cos(\gamma) \\ &\quad +sin(\beta) \cdot cos(\gamma) - sin(\beta) \cdot cos(\alpha) \\ &\quad +sin(\gamma) \cdot cos(\alpha) - sin(\gamma) \cdot cos(\beta) \end{aligned} \tag{6}$$

with:

$$Y = \frac{Y_n}{D}, \qquad U = \frac{U_n}{D}, \qquad V = \frac{V_n}{D} \tag{7}$$

As such, a decoder can be implemented that is able to decode the Y, U, and V components directly from three composite samples encoded at non-equal sub-carrier phases α, β and γ. This is shown as a block diagram in Figure 5. As before, with *non-identical* Y, U and V values, perfect separation is not possible and errors in the decoded values will occur.

2.2. Noise robustness

Indeed, experiments confirm the validity of the above decoding principle, but have also shown that noise robustness depends upon the sub-carrier phases of the input samples. In this context, noise refers to both transmission noise as well as the imperfect correlation of input samples. Due to both factors, the above decoding will result in errors.

By means of an experiment, the noise robustness as function of the sub-carrier phases of the input samples was determined. The experiment was performed by adding a noise with a known characteristic to the input samples, and then determining the signal-to-noise ratio (SNR) of the decoded output samples. By varying the sub-carrier phases α, β and γ independently, all possible phase combinations can be tested. However, in order to reduce complexity, the noise robustness can be sufficiently characterized by only two measurements with two variables instead of the exhaustive testing of three variables, as shown in Figure 6.

In the first measurement, the phase α of one of the three samples is set to 0°, whereas the phases β and γ of the remaining samples vary from 0° to 360°. In the second measurement, the absolute phase α of one of the three samples varies from 0° to 360°, whereas the relative phase $\pm\beta$ of both remaining samples increases from 0° to 180°. As such, it allows for a determination of the optimum *relative* phases as well as any dependency upon the *absolute* phases of the composite samples.

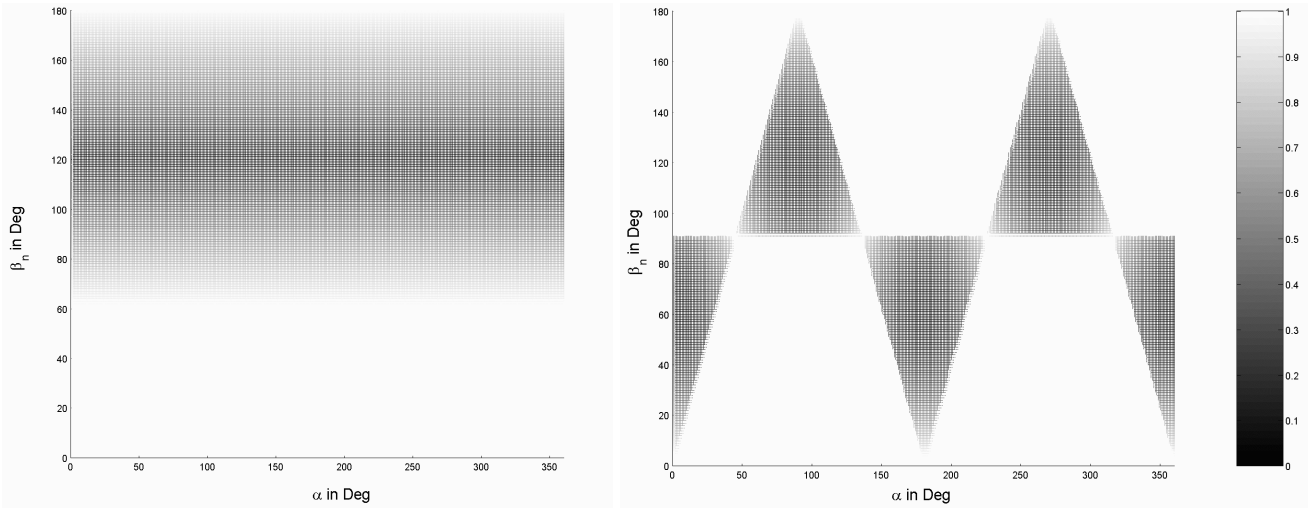

Figure 7. Normalized luminance noise level as a function of the absolute phase α for one sample, and the relative phases β and $-\beta$ for the remaining samples, for a) identical V-switches, and b) non-identical V-switches. The gray-scale intensity indicates the noise corruption (zero corresponds to no noise corruption).

An example of the first measurement for samples with identical V-switches is shown in Figure 7a. Here, the noise corruption of the decoded luminance component is given at a phase combination α for the first sample, β for the second sample and $-\beta$ for the third sample. From this, two observations can be made. First of all, clearly the noise robustness does not depend on the absolute phase α, but only on the phase differences β. Secondly, the highest noise robustness is achieved around phase differences of 120°, e.g. $(\alpha, \beta, \gamma) = (0°, 120°, 240°)$.

Similarly, Figure 7b shows an example of the second measurement for samples with non-identical V-switches. Contrary to the situation with identical V-switches, the noise robustness is now dependent upon the absolute phase α of the sample with the unequal V-switch. This means that the optimum relative phase difference β varies as a function of the absolute phase α. For example, if α is 180°, the ideal relative phase differences now equal approximately ±60°, i.e. $(\beta, \gamma) = (120°, 240°)$ or $(\beta, \gamma) = (240°, 120°)$.

These results are similar to the classical decoding using two samples with opposite phases, as again the optimum sub-carrier phases depend upon the V-switches of the input samples. However, the new decoding principle allows for larger phase deviations without a significant reduction in noise robustness. In contrast, the phase requirements for the classical decoding are far more strict, as even with noise-free input signals, only an opposite relative or absolute phase will yield noise-free output signals.

3. IMPLEMENTATION OF THE NEW DECODER

We now have two methods available for decoding, i.e. using two samples with opposite phases, as described in Section 1.2, and a new method using three samples with non-opposite phases, as described in Section 2. Combining both methods promises an increase in decoding quality, as in some situations a three sample filter is expected to yield better results than a two sample filter and vice versa. By locally selecting the filter that yields superior results, an overall increase in quality is expected. This means that, instead of adaptively combining a limited number of fixed decoding options, samples are used that exhibit the highest correlation regardless of their exact spatial or temporal direction.

3.1. Principles

As such, decision rules are required that, based upon local signal characteristics, select the most suitable decoding option. In our approach, this decision is performed on a per-sample basis, i.e. for every composite sample to be decoded, the most suitable filter is chosen. In turn, the filter's suitability is determined by the samples in its aperture.

The most suitable sample for either decoder is primarily determined by the expected correlation, as insufficiently correlated samples yield decoding errors. However, the phase requirement is important as well, as for the two sample decoder, only samples which have an opposite phase can be used for comb-filtering. For the three sample decoder, the phase requirements are more complicated, as some phase combinations are significantly less noise robust than others (see Figure 7).

With both phase and correlation information available, a straightforward approach is to apply both criteria to spatially and/or temporally adjacent samples: the so-called *candidate set*. The optimum samples or *candidates* within that candidate set serve as input to either the two or three sample filter, thereby decoding the current composite sample. In order to account for both constraints, we can apply a penalty to each candidate within the candidate set according to:

- *Optimum phase relationship between samples* in order to achieve the highest noise robustness.
- *Highest correlation between samples* in order to minimize correlation noise.

However, determining the correlation between samples constitutes a chicken-or-the-egg problem: in order to decode the composite video, one needs to know the correlation between samples, which in turn is only available after decoding. To break this cycle, the decoder can be initialized by a simple separation, i.e. the band-pass and notch filters as depicted in Figure 2. Even though this initial separation is far from perfect, experimental validation has shown its suitability for this purpose.

3.2. Candidate set

In our approach, the candidates are obtained from a rectangular window around the current sample. The exact size of the candidate window is determined by the horizontal and vertical boundaries t_x and t_y, as shown in Equation 8. Again, $F(\vec{x}, n)$ is the composite sample at the pixel position $\vec{x}$ in a given field n.

$$C(\vec{x}, n+m) = \left\{ F(\vec{x} + \begin{pmatrix} i \\ j \end{pmatrix}, n+m) \right\} \tag{8}$$

with:

$$i \in \{-t_x, \ldots, t_x\}, j \in \{-t_y, \ldots, t_y\}$$

If only spatial candidates are used, i.e. $m = 0$, this leads to Equation 9, i.e. the complete candidate set CS equals the spatial candidate set $C(\vec{x}, n)$.

$$CS = \{C(\vec{x}, n)\} \tag{9}$$

However, CS might be composed of spatial as well as temporal candidates. For example, consider the candidate set shown in Equation 10 and Figure 8a, where candidates originate from candidate windows in the previous, current and next field.

$$CS = \{C(\vec{x}, n+1), C(\vec{x}, n), C(\vec{x}, n-1)\} \tag{10}$$

As opposed to temporal windows centered around the current spatial position, motion compensation could be used to increase the correlation of temporal candidates by positioning the candidate windows along the motion

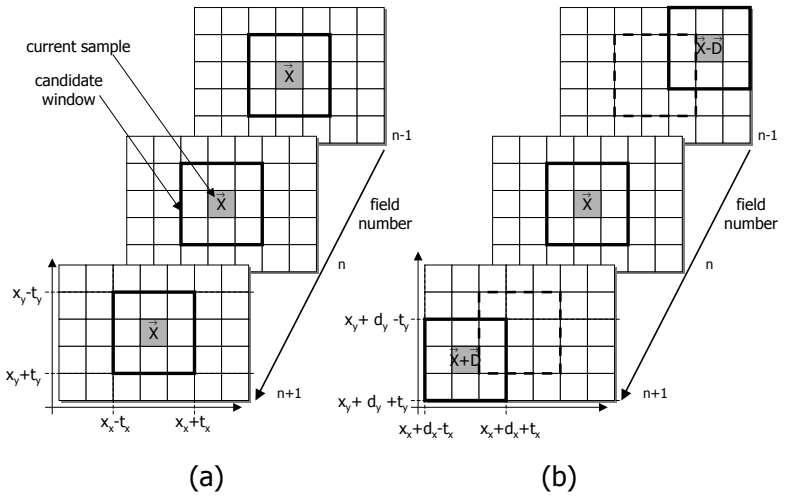

Figure 8. Candidate windows in the next, current and previous fields at a) fixed position $\vec{x}$ and b) motion compensated positions $\vec{x} + D(\vec{x}, n)$, $\vec{x}$ and $\vec{x} - D(\vec{x}, n-1)$ respectively.

axis. This is illustrated in Equation 11 and Figure 8b, where $D(\vec{x}, n)$ describes the displacement of the sample at pixel position $\vec{x}$ in field n to field $n+1$ (the displacement from field n to $n-1$ is assumed to be $-D(\vec{x}, n)$, i.e. linear movement).

$$CS = \left\{ \begin{array}{l} C(\vec{x} + D(\vec{x}, n), n+1), \\ C(\vec{x}, n), \\ C(\vec{x} - D(\vec{x}, n), n-1) \end{array} \right\} \tag{11}$$

Due to the increase in latency, decoders using a next field can be undesirable. Therefore, various configurations are possible using only previous fields. For example, the following candidate sets can be used for frame and field, field only and frame only decoders, respectively:

$$\begin{aligned} CS &= \{C(\vec{x}, n), C(\vec{x}, n-1), C(\vec{x}, n-2)\} \\ CS &= \{C(\vec{x}, n), C(\vec{x}, n-1)\} \\ CS &= \{C(\vec{x}, n), C(\vec{x}, n-2)\} \end{aligned} \tag{12}$$

3.3. Penalty functions

Given a candidate set CS of $CSMAX$ candidates, a penalty value is assigned to each candidate as a function of both the phase relationship and the correlation to the current sample. This is shown in Equation 13, where the penalty ϵ_i is calculated for all candidates CS_i with $i \in \{1, \ldots, CSMAX\}$. The total penalty equals the weighted sum of the *correlation penalty* $L(CS_i, F_{cvbs1})$ and the *phase penalty* $P(CS_i)$:

$$\epsilon_i(CS_i, F_{cvbs1}) = \alpha_1 \cdot L(CS_i, F_{cvbs1}) + \alpha_2 \cdot P(CS_i) \tag{13}$$

Here, α_1 and α_2 correspond to experimentally determined weighting factors, and F_{cvbs1} is the current composite video sample.

The correlation penalty is calculated in a straightforward manner as the absolute difference of the initially separated luminance values, as shown in Equation 14. Experiments verified the validity of this approach, although improvements may be achieved using a more elaborate penalty function.

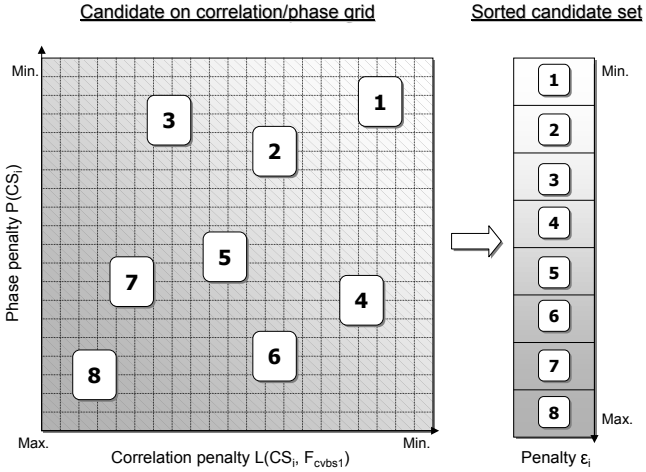

Figure 9. Candidates on a 2D correlation/phase plane and the resulting sorted candidate set.

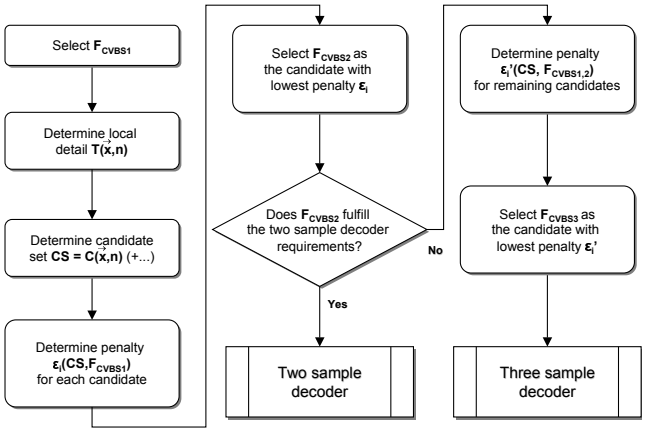
Select F_CVBS1
Determine local detail T(x,n)
Determine candidate set CS = C(x,n) (+...)
Determine penalty ε_i(CS,F_CVBS1) for each candidate
Select F_CVBS2 as the candidate with lowest penalty ε_i
Does F_CVBS2 fulfill the two sample decoder requirements?
No
Yes
Two sample decoder
Determine penalty ε_i'(CS, F_CVBS1,2) for remaining candidates
Select F_CVBS3 as the candidate with lowest penalty ε_i'
Three sample decoder

Figure 10. Flowchart of the new decoder.

$$L\left(CS_i, F_{cvbs1}\right) = |Y_{init}(F_{cvbs1}) - Y_{init}(CS_i)| \tag{14}$$

The phase penalty is based upon the principle that the phase differences that result in the highest noise robustness should yield the lowest penalty. For the two sample filter, the desired phase difference are 180° or an opposite absolute phase depending upon the V-switch, and as such, these yield no penalty. In turn, differing phase combination will have a large penalty. For the three sample filter, the required phase differences correspond to those that yield the highest noise robustness in Figure 7. Hence, the penalty function is based upon an approximation of these noise measurements.

3.4. Candidate selection

After determining the penalties for the $CSMAX$ candidates within candidate set CS, the optimum candidate, i.e. the one with the lowest penalty, will be chosen according to Equation 15. This is also shown in Figure 9, where a number of candidates are shown on a 2D correlation/phase plane, as well as the resulting sorted candidate set.

$$\begin{aligned} \exists j \in [1, \ldots, CSMAX] : \forall i \quad &\in \quad [1, \ldots, CSMAX] : \epsilon_j \leq \epsilon_i \\ F_{cvbs2} \quad &= \quad CS_j \end{aligned} \tag{15}$$

In the following two situations, both samples will be decoded by the two sample decoder:

- The V-switch of F_{cvbs1} and F_{cvbs2} is *equal*, and both samples have an opposite relative phase (i.e. phase difference 180°).
- The V-switch of F_{cvbs1} and F_{cvbs2} is *opposite*, and both samples have an opposite absolute phase.

In all other cases, no suitable candidates for the two sample decoder was available, and as such, F_{cvbs_2} has been optimized for the three sample decoder: a third sample is now required with an optimum phase relationship and correlation to both F_{cvbs1} and F_{cvbs2}. Therefore, a modified penalty ϵ_i' is determined for all remaining candidates, after which F_{cvbs3} is selected as the candidate with the lowest penalty. This process is shown as a flowchart in Figure 10.

A potential drawback of above candidate selection is that the suitability of a candidate for F_{cvbs2} determines the choice between the both decoders. It may occur that the three sample decoder is chosen due to a more suitable candidate for F_{cvbs2}, while no suitable candidate for F_{cvbs3} can be found. In this case, the two sample decoder potentially yields better decoding quality. This can be avoided by taking the correlation of all candidates into account. However, this is computationally expensive, as it requires the exhaustive testing of all possible candidate combinations.

In conclusion, the above penalty calculation determines the penalty as a function of both the correlation as well as the phase difference. The optimum phase difference yields no phase penalty, whereas an unsuitable phase difference results in the maximum phase penalty. This ensures that candidates with the best correlation and optimum phase differences will be selected as input samples. Based on the suitability of these input samples, the corresponding filter is then selected.

3.5. Decoder configurations

The above decoding principles can now be applied to decode the composite video signal into Y, U and V components. Typically, the decoded chrominance components are then low-pass filtered to suppress frequency components above approximately 1.3MHz. This is possible since the chrominance has been bandlimited prior to encoding. As such, any high frequent decoding errors and/or noise can be suppressed, as clearly they cannot be part of the original chrominance signal. Furthermore, various optional enhancements can be applied. Below is a brief selection of enhancements that have shown to yield an improved decoding quality:

Up-sampling to a spatially denser grid can be used. Within a certain spatial distance, now k times as many candidates are available in comparison to the original sampling grid (with k being the up-sampling factor). Therefore, the amount of candidates has increased, whereas a deterioration of correlation due to increased spatial distance has been avoided.

Vector median filtering[7] can be applied to the top m decoder outputs. The result is that the output of the decoder with the least extreme value is selected. As such, outliers are removed and do not contribute to the output. The influence of decoding errors in the output will therefore be attenuated.

Deriving luminance from decoded chrominance can also be used to suppress decoding errors. Unlike the luminance signal, the chrominance signal is strictly bandlimited prior to encoding. As such, any high-frequency components are caused by decoding errors and/or noise, and can be suppressed by applying a low-pass filter. The obtained clean chrominance signal can then used to obtain an improved luminance signal by remodulating the chrominance and subtracting it from the composite signal.

Recursive decoding can be used to improve upon the estimation of the correlation between samples. As the notch-filter initialization is far from perfect, a significant improvement in decoding quality can be achieved by using a more elaborate filter. One way of doing so is recursive decoding, where the previous decoder output is used to initialize repeated decoding passes. However, due to the required causality, an initial separation of the composite signal is still required.

4. EVALUATION OF THE NEW DECODER

The quality assessment of the new decoder was performed by means of *subjective* as well as *objective* quality measures. The subjective evaluation was primarily done by split-screen comparisons of moving sequences as well as still fields. The evaluation was an informal subjective test, i.e. not compliant to any standard testing procedure (e.g. ITU-R BT.500-10).

For the objective assessment, the Mean Square Error (MSE) was used as criterion to measures the difference between the reference and the decoded image. Here, the MSE between the decoded signal F_{dec} and the reference signal F_{ref} is defined as:

$$MSE(n) = \frac{1}{N} \sum_{\vec{x}} \left(F_{ref}(\vec{x}, n) - F_{dec}(\vec{x}, n) \right)^2 \tag{16}$$

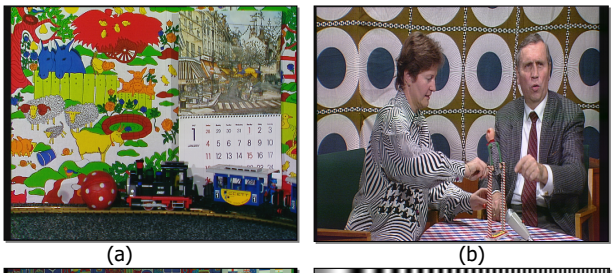

Figure 11. Snapshots of the test sequences: a) *Mobile calendar*, b) *Cross-color couple*, c) *Shopping zoom* and d) *Moving zoneplate* (visible alias is due to printing, and not part of the actual sequence).

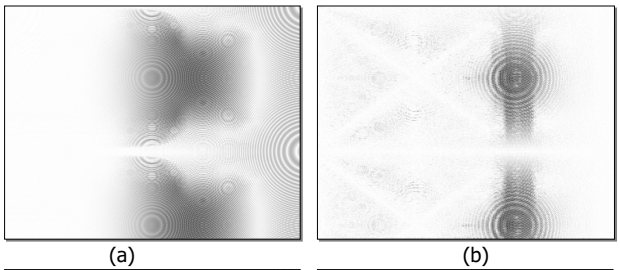

Figure 12. Decoded *Moving zoneplate* of a) reference 2D[0], b) proposed 2D[0], c) reference 3D[-1,0] and d) proposed 3D[-1,0] comb filters.

with N being the number of pixels within a field n and $\vec{x}$ the current sample's position. In our case, the MSE was determined for both the luminance and the chrominance, and averaged over multiple fields. As the pre-filtered signals prior to encoding were chosen as a reference, an ideal comb-filter will yield a zero MSE.

A number of test sequences were selected to evaluate the performance of the comb-filters using the mentioned assessment methods. Ideally, the content of these test sequences should be representative for common broadcast video. However, as this requires an extensive set of sequences, the choice was limited to those where severe cross-talk artifacts were expected to occur. This excludes sequences containing little high-frequency content, e.g. blurry or smooth images. The final test set included, amongst others, the sequences depicted in Figure 11.

In order to benchmark the performance of the proposed comb-filter, the following filters were selected as reference:

1D Band-pass/notch filters, as they are still widely used in low-end televisions.

2D Spatial median filter, that combines various spatial comb filters by means of a median filter.

3D Motion adaptive filter, that switches between temporal and spatial filtering depending upon the local amount of motion. Two configurations for temporal filtering were used: a field-comb-filter (3D$[-1, 0]^*$) and a frame-comb-filter (3D$[-4, 0]$).

The results of an objective evaluation are shown in Table 1. Furthermore, Figure 12 illustrates the luminance error when decoding the *Moving Zoneplate* sequence. Combined with the subjective impressions, we can conclude that the proposed filters achieve an increase in sharpness and reduction of cross-color artifacts compared to the reference filters. The gain in cross-luminance reduction, however, is less significant due to the filter's color-blindness, which particularly results in artifacts around strong chrominance edges without accompanying luminance transition. As chrominance edges typically do coincide with luminance edges, the above situation is unlikely to occur in common broadcast video.

*The index refers to the fields used by the comb-filter. For example, the 3D$[-1, 0, +1]$ comb-filter obtains candidates from the previous, current and next fields.

Sequence		Reference				New decoder			
	Y/UV	Notch	2D[0]	3D[-1,0]	3D[-4,0]	2D[0]	3D[-1,0]	3D[-1,0,+1]	MC-3D[-1,0,+1]
Mobile	Y	73.6	52.1	50.2	70.4	40.8	31.9	28.0	27.4
calendar	UV	39.3	33.5	29.5	29.7	31.5	25.7	23.2	23.1
Cross-color	Y	91.7	61.1	59.7	54.2	43.6	29.0	23.5	23.2
couple	UV	39.2	24.0	17.4	17.0	25.9	17.6	14.6	14.5
Shopping	Y	57.2	46.4	35.6	52.3	37.2	30.2	27.4	26.7
zoom	UV	36.2	36.7	33.3	32.4	32.7	28.1	25.5	25.5

Table 1. MSE comparison using *Mobile calendar*, *Cross-color couple* and *Shopping zoom* sequences.

Furthermore, the 2D filter configuration of the proposed decoder is able to achieve similar performance as the 3D reference comb filters. This is particularly interesting, as a high cost is associated with temporal filters due to the requirement of one or even multiple field memories. However, further tests have shown that the demonstrated improvement becomes less in case of strong noise corrupted sequences. As such, further work is required to further increase the noise robustness.

5. CONCLUSIONS AND FURTHER WORK

The proposed decoder enables the Y/C separation of samples with non-opposite chrominance phases. This provides additional decoding options to decoders. Our experience shows that the combination of both filters in the proposed decoder yields better results than typical current high-end comb filter. In our paper, we also introduced various other techniques that can be applied to further increase the decoding quality, such as spatial upsampling and recursive decoding.

Further research could improve the noise robustness to ensure a similar performance gain in noise-corrupted as in noise-free video signals. For that purpose, combination with advanced noise suppression techniques could be evaluated. Although it has been established that the inclusion of the proposed filter significantly improves decoding quality, the implementation cost should be balanced against the achievable quality gain.

REFERENCES

1. K. Jack, *Video demystified: a handbook for the digital engineer, 3rd ed.*, LLH Technical Publishing, Eagle Rock, 2001.
2. D. Teichner, "Quality improvement by adaptive inter-/intraframe processing in PAL TV receivers", *IEEE Trans. Consumer Electron.* **31**, pp. 226-239, 1985.
3. D. Teichner, "Adaptive filter techniques for separation of luminance and chrominance in PAL TV signals", *IEEE Trans. Consumer Electron.* **32**, pp. 241-250, 1986.
4. D. Teichner, "Three-dimensional pre- and post-filtering for PAL TV signals", *IEEE Trans. Consumer Electron.* **34**, pp. 205-227, 1988.
5. I.T. Briggeman, *Motion-compensated Y/C-separation of the composite PAL video signal, Graduation Thesis*, Delft University of Technology, Delft, 1990.
6. S. Choi and S. Kwon, H. Kim, Y. Kwon, Y. Ha, "Motion adaptive 3D Y/C separation algorithm using motion estimation and motion compensation", *IEEE Trans. Consumer Electron.* **47**, pp. 770-778, 2001.
7. J. Astola and P. Haavisto, Y. Neuvo, "Vector Median Filters", *Proc. IEEE* **78**, pp. 678-689, 1990.